RESEARCH ARTICLE

INTERNATIONAL MICROBIOLOGY (2014) 17:235-247
doi:10.2436/20.1501.01.226 ISSN (print): 1139-6709. e-ISSN: 1618-1095
www.im.microbios.org

INTERNATIONAL MICROBIOLOGY
OPEN ACCESS

Ignimbrite textural properties as determinants of endolithic colonization patterns from hyper-arid Atacama Desert

Beatriz Cámara[1]*, Shino Suzuki[2], Kenneth H Nealson[2,3], Jacek Wierzchos[1], Carmen Ascaso[1], Octavio Artieda[4], Asunción de los Ríos[1]

[1]National Museum of Natural Sciences-CSIC, Madrid, Spain. [2]J. Craig Venter Institute, La Jolla, CA, USA. [3]University of Southern California, Los Angeles, CA, USA. [4]Department of Plant Biology, Ecology and Earth Sciences. University of Extremadura, Plasencia, Spain

Received 23 September 2014 · 15 December 2014

Summary. This study explores the photosynthetic microbial colonization of rhyolitic ignimbrites in Lomas de Tilocalar, a hyper-arid region of the Atacama Desert, Chile. Colonization appeared in the form of a green layer a few millimeters beneath the ignimbrite surface. Some ignimbrite rocks revealed two distinct micromorphological areas of identical mineralogical and chemical composition but different textural properties. According to texture, colonization patterns varied in terms of the extension and depth of colonization. The diversity of photosynthetic microorganisms was assessed by denaturing gradient gel electrophoresis (DGGE) of the 23S rRNA gene and by generating clone libraries of the 16S rRNA gene. We observed a low diversity of photosynthetic microorganisms colonizing the ignimbrite microhabitat. Most rRNA gene sequences recovered greatly resembled those of *Chroococcidiopsis* hypolith clones from arid deserts. These results point to highly restrictive conditions of the hyper-arid Atacama Desert conditioning the diversity of cyanobacteria, and suggest that microbial colonization and composition patterns might be determined by the microscale physico-chemical properties of the ignimbrite rocks. [**Int Microbiol** 2014; 17(4):235-247]

Keywords: *Chroococcidiopsis* sp. · endoliths · ignimbrite · rock porosity · volcanic rock · Atacama Desert

Introduction

Microbial communities in terrestrial volcanic environments have been scarcely investigated despite the wide distribution of highly colonized volcanic rocks on Earth (approximately 95% of the Earth's crust) [2,13,23,30]**.** Most microbiological studies have been conducted almost exclusively in volcanic regions of Iceland where temperatures are low and snow covers the ground during most of the year [12,31,32,36–38]. Many such studies have linked the diversity of microbial communities in volcanic environments to rock geochemistry and have centered on identifying the effects of diversity on weathering and soil neogenesis [12,38]. This type of characterization study is essential to understand the potential roles of these microorganisms in the weathering processes that contribute to the global carbonate-silicate cycle [11,12,32,36].

The geochemical (chemical and mineralogical composition) and textural (size, crystal shape and organization, mineral and matrix porosity) properties of rocks determine how susceptible, or bioreceptive, a rock is to colonization by different microorganisms and organisms [27,44]. In particular, the movement of water through the rock matrix is conditioned

*Corresponding author: B. Cámara
Museo Nacional de Ciencias Naturales-CSIC
Serrano, 115 bis
28006 Madrid, Spain
Tel. +91-7452500. Fax: +91-5640800
E-mail: beacamara@gmail.com

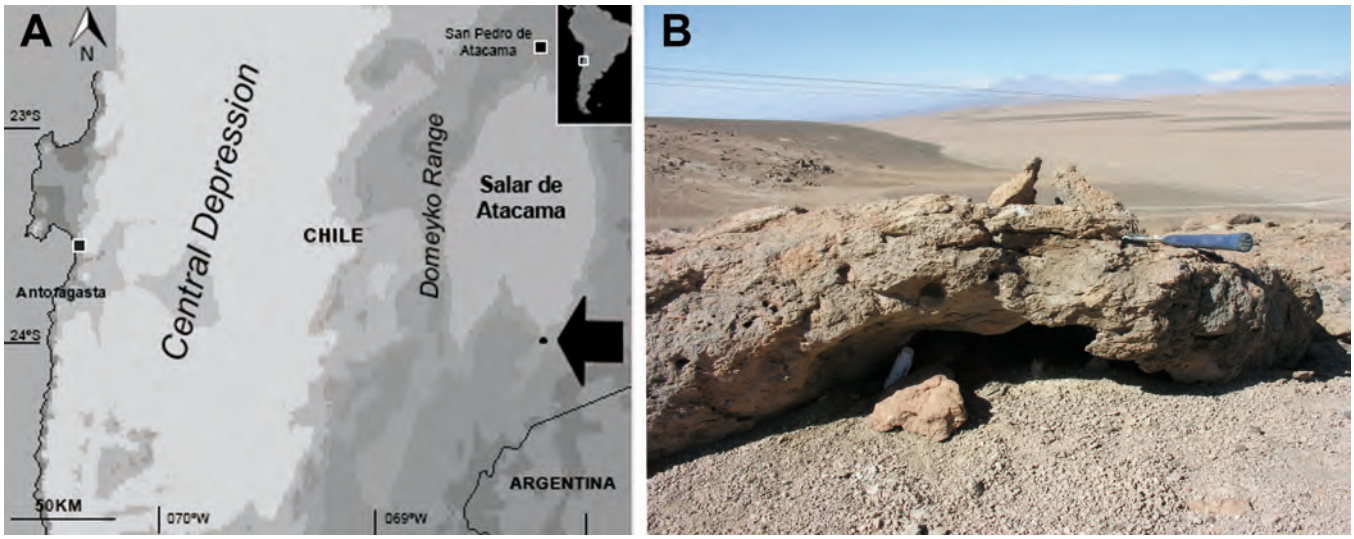

Int Microbiol

Fig. 1 (**A**) Map showing the geomorphic units of central Atacama Desert and the study area (arrow), south of the Salar de Atacama basin. (**B**) Landscape of the sampling site in Lomas de Tilocalar showing the location of the microweather station and Pliocene Tucucaro ignimbrite rocks on a typical N-S trending ridge.

by the physical properties of the rock (e.g., pore size, pore connectivity, permeability, water absorption kinetics, or water retention capacity) and this, in turn, will determine its microbial colonization capacity [44,58]. Other factors such as pH, level of exposure to climate and nutrient sources are also known to influence the bioreceptivity of rocks [16,46].

So far, various groups of microorganisms have been observed to inhabit volcanic rocks featuring a variety of mineralogical, chemical and textural properties [2,12,23,31,32, 36–38]. Among these, cyanobacteria play an important role in rock weathering via their capacity to extract bio-essential elements from rocks by increasing the pH of their surroundings [7]. Further, in a controlled laboratory experiment, both cyanobacterial growth and weathering rates of colonized volcanic rocks were found to be affected by the chemical and mineralogical composition of the rock. Thus, basalt rocks (highly essential element levels) showed higher rates of cyanobacterial growth and substrate dissolution than rhyolitic rocks (high silica levels) [45]. These observations have revealed that the physico-chemical properties of rocks determine the metabolic activity of microorganisms, and that, vice-versa, rocks can also be modified by the activities of their colonizing microorganisms [31,59].

The Atacama Desert features extensive areas covered with felsic lava flows arising from volcanic activity in the Andes [4,26]. Ignimbrite structures dominate the Preandean Depression and Altiplano areas of this desert and are thought to have formed in the Pliocene and Upper Miocene as a result of pyroclastic flows erupted from large boiler systems in the Altiplano area, east of the Salar de Atacama [17,21]. Recently, Wierzchos et al. [62] detected microbial communities inhabiting ignimbrites in the Preandean Depression area. These authors have proposed that the volcanic rock interior protects endolithic cyanobacteria and associated heterotrophic bacteria against the intense UV radiation and high visible light levels that prevail in this region. This study served to broaden the spectrum of rock substrates known to act as lithic microhabitats for microorganisms in the hyper-arid region of the Atacama Desert, namely ca-sulfate crusts [63], halite [15,52], quartz rocks [40] rock-varnish [39], rhyolite-gypsum, and calcite rocks [18], and finally, ignimbrite rocks [62].

This study examines the diversity of photosynthetic bacteria that colonize two texturally different areas of rhyolitic ignimbrite rocks in the hyper-arid Atacama Desert. Its objective was understanding why these two habitats show different patterns of microbial diversity given their similar chemistry, yet different microstructure. Microbial diversity was examined through DGGE and clone libraries of 23S rRNA and 16S rRNA gene sequences. The textural properties of rocks were determined using several microscopy and analytical procedures.

Materials and methods

Site description and sampling. The study site was Lomas de Tilocalar (23º57′25″S, 68º10′12″W and 2986 m asl), south of the Salar de Atacama basin in the eastern region of the Atacama Desert (Chile) (Fig. 1A). This area shows a N-S trending depression facing eastward towards the Cordon de Lila range, along with several subparallel N-S trending ridges topped with Plio-

cene Tucucaro ignimbrite (3.2 ± 0.3 Ma, Fig. 1B) [24,26,51]. A detailed description of the area and its microclimate (for the period 20 March 2010 to 23 September 2011) may be found in Wierzchos et al. [62]. The site, featuring extremely low rainfall and a high evapotranspiration rate, is classified as hyper-arid (aridity index ~ 0.0075). Over the period specified above, mean annual temperature was 14.4ºC with a maximum of 37.5 ºC and minimum of –7.4 ºC. Relative humidity was exceptionally low, the annual mean being 16.2%, and ranging from 1 to 95.3%. Precipitations consisted of occasional rainfall events (22 mm/yr in 4 separate episodes) as the only source of liquid water in this area.

In 2010, samples of ignimbrite rocks were randomly collected with the help of a hammer and a chisel 3–10 m from the microclimate station Onset HOBO Weather Station Data Logger (Onset Computed Company, Bourne, MA, USA). Fracturing exposed a visible green band of endolithic colonization. The ignimbrites sampled originated from pyroclastic flows consisting of gas, ash and lava deposited chaotically while still hot. This means that post-depositional flow likely gave rise to the typical texture of ignimbrite containing flat pumice fragments. The Tucucaro ignimbrite [51] collected for this study is beige or dark (indicated as zone IgD in Fig. 2A,B), and features flat pumice fragments (indicated as IgW-white zone in Fig. 2A,B). Note that the green band of endolithic colonization appears continuous from one zone to the other in ignimbrite rocks showing this IgD/IgW interface. Thus, we searched for this feature by fracturing rocks, though the task was challenging because of the scarcity of rocks showing this continuous green band. The collected rock fragments were sealed in sterile zip-lock bags (Whirlpark, Fisher Scientific) avoiding any hand contact. Samples were transported stored dry in the dark at ambient temperature. Once at the laboratory (within 20 days), they were immediately processed.

X-ray diffraction (XRD) and X-ray fluorescence spectroscopy (XRF). The mineralogical composition of IgD and IgW was determined by X-ray powder diffraction, using a Philips X′ Pert diffractometer PW 1830 for polycrystalline samples with a graphite-monochromated CuKα radiation source (Cu cathode of wavelength Kα = 1.54051). Samples were ground to a particle size ≤40 μm and this powder was used to obtain the XRD diffractograms. For qualitative analysis of the crystalline phases present in the samples, the Power Diffraction File (PDF-2, 1999) of the International Centre for Diffraction Data (ICDD) was used. A semi-quantitative analysis of these phases was performed using the normalized reference intensity ratio (RIR) method [10] using RIR values for each phase from the powder diffraction database (ICDD). Quantitative chemical composition in terms of major and minor elements was determined by X-ray fluorescence (XRF) spectroscopy. XRF spectra for the ignimbrite rock fragments were acquired using a Philips PW-1404 spectrometer with Sc-Mo X-ray tube and scintillation gas (PR- 10) detector, after milling in an agate mortar. For analytical data treatment, we used Super-Q Manager Geostandards software (CRNS, France).

Polarized light microscopy. The petrographical study of the two differentiated areas of ignimbrite rocks was conducted on thin sections (30 μm thick) examined using a Nikon Eclipse LV100 Pol polarized light microscope (PLM) equipped with a Nikon DS-Fi1 digital camera.

Scanning electron microscopy in back-scattered electron mode (SEM-BSE). Ignimbrite rocks showing the IgD/IgW interface were processed for their examination by SEM-BSE following Wierzchos & Ascaso [61]. Briefly, samples were dehydrated and embedded in LR-White resin, finely polished and carbon coated. Finally, the polished surfaces of rock-embedded samples were observed in a Zeiss DMS 960 SEM microscope equipped with a four-diode, semiconductor BSE detector and ISIS Link EDS (Energy-Dispersive X ray Spectroscopy) microanalytical system under the conditions: 0º input angle, 35º output angle, 15 kV acceleration potential, 6–15 mm working distance and 5–10 nA probe current.

Mercury intrusion porosimetry (MIP). The pore systems of the IgD and IgW zones were characterized by mercury intrusion porosimetry in terms of their connected porosity, pore size distribution and mean pore size according to Benavente et al. [5]. The equipment used was a PoreMaster 60/Quantachrome instrument to determine porosity (connected porosity) of the rock samples in the range of pore diameters 0.00036 μm to 190.58 μm. In the Washburn equation, a mercury surface tension of 0.48N/m was used, and a rock-mercury contact angle of 140 dag was used in the Laplace equation. Porosity (total porosity %) was then determined as the weight-normalized volume of mercury intruded in the sample.

DNA extraction. Sample preparation for denaturing gradient gel electrophoresis (DGGE). Ten colonized fragments of ignimbrite rock showing the IgD/IgW interface were used for this study. Given the low volume of colonized material in each ignimbrite rock, material from several rocks was mixed to provide 100-mg samples for DNA extraction. Three different pooled samples of each texture (IgD-I, IgD-II, IgD-III and IgW-I, IgW-II, IgW-III) were processed for DGGE analysis. The colonized material was collected using a sterile blade from the fresh green band of ten rock fragments. Prior to DNA extraction, the rock material was frozen in liquid nitrogen and then pulverized with the aid of a sterile micropestle (Eppendorf micropestle, Sigma-Aldrich). Total genomic DNA was extracted using the UltraClean Microbial DNA Isolation kit (Mobio Laboratories, Solana Beach, CA, USA) according to the manufacturer's instructions.

Sample preparation for the construction of clone libraries. Two pooled rock samples were prepared to construct a clone library representative of each ignimbrite zone (IgD and IgW) as described above for the DGGE samples. Total genomic DNA was extracted using the Ultraclean® Soil DNA Isolation Kit (Mobio Laboratories Inc., Carlsbad, CA, USA) following the manufacturer's instructions.

For both analyses, the quality and quantity of the total genomic DNA extracted was determined in a NanoDrop spectrophotometer 1000 (Thermo Scientific, Waltham, MA, USA). Genomic DNA (*ca.* 10–50 ng) was used for PCR amplification with different genetic markers.

Denaturing gradient gel electrophoresis (DGGE) of the 23S rRNA gene. To obtain a quick overview of photosynthetic microbial composition, the endolithic colonization of IgD and IgW in the prepared samples was analyzed by denaturing gradient gel electrophoresis (DGGE). Total genomic DNA from samples IgD-I, IgD-II, IgD-III and IgW-I, IgW-II, IgW-III was used for PCR amplification using specific primers for phototrophs: p23SrV_f1_GC and p23SrV_r1. These primers flank domain V of the 23S rRNA gene, a hypervariable region of this gene (~400 bp) only present in cyanobacteria and plastids, and can discriminate among taxa at the species levels [55]. The PCR and thermal cycling conditions used were as described by Sherwood & Presting [55]. The PCR products obtained from zones IgD and IgW were separated on a D-Code Universal Mutation Detection System (BioRad, Hercules, CA, USA) using 6% acrylamide/bisacrylamide gel (37.5:1) on a 30–70% denaturing gradient of urea-formamide (where 100% is defined as 7 M urea and 40% v/v). Electrophoresis was carried out in 1X TAE buffer at 100 V and 60°C for 16 h. The predominant DGGE bands (in terms of intensity and frequency) were excised using a sterile scalpel, and incubated in sterile distilled water overnight at 4°C. Next, the DGGE bands were reamplified under the same PCR conditions using the same primer pair as described above, but this time without the GC clamp. The identity of the new PCR products was verified by comparing their electrophoretic positions with the original positions of the other bands in the DGGE gel. PCR products were sequenced at the Macrogen Company sequencing service (Seoul, South Korea). Phylotypes were determined based on sequence similarity ≥99%. All DGGE band sequences obtained were deposited in GenBank (KP238376–81).

Construction of 16S rRNA gene clone libraries.Total genomic DNA from IgD and IgW samples was used for PCR amplification of the 16S ribosomal RNA gene using the following set of primers for eubacteria: specific primer U27f and universal primer U1492r [41]. Each 25 µl reaction mixture contained 0.625 U of Taq polymerase *TaKaRa Ex Taq* 5U/µl (Takara Bio Inc.), 0.2 mM of each of the four dNTPs, 0.2 µM of each primer (10 mM), 2.5 µl *Ex Taq Buffer* (10X) (Mg^{2+} free), 2 µl of DNA template (~10–50 ng) and sterile bidistilled water up to a volume of 25 µl. The PCR conditions were an initial denaturation step at 94°C for 2 min, followed by 30 cycles of denaturation at 94°C for 30 s, annealing at 55°C for 30 s, extension at 72°C for 1 min and 30 s, and a final extension phase of 72°C for 7 min. The purified PCR products (~1400 bp) were then used to construct one clone library for each sample (IgD and IgW). To this end, the purified products were ligated into the pGEM-T vector (pGEM®-T Easy Vector System kit, Promega®) according to the supplier's instructions, and subsequently introduced into *Escherichia coli* JM109 competent cells (Promega, USA). After incubation at 37°C for 18 h, approximately 50 white colonies were randomly selected from each genomic library, purified and used as DNA template in the insert PCR reaction using primers M13F and M13R. For this, a reaction volume of 25 µl was prepared following the protocol described above. The PCR products containing the insert (~1700 bp) were purified and sequenced on an ABI DNA sequencer 3730xl (Applied Biosystems, Carlsbad, California, USA) and the resulting chromatograms analyzed using the software FinchTV 1.4.0 [www.geospiza.com/FinchTV]. Chimeras were identified using the Bellerophon server [http://comp-bio.anu.edu.au/Bellerophon/doc/doc.html] [33] with the Huber-Hugenholtz correction and a window size of 300 bp as selected parameters. Remaining sequences were clustered in operational taxonomic units (OTUs) using MOTHUR software [http://www.mothur.org/] [54]. OTUs were defined as showing 95% sequence similarity (cutoff 0.05) for the genus level and 97% sequence similarity (cutoff 0.03) for the species level [53], using the furthest-neighbor algorithm at an accuracy of 0.01. The resulting 16S rRNA gene sequences were deposited in GenBank (KP238382-411). Finally, library coverage was estimated as a measure of the sampling effort. Also calculated were the variables Shannon's index (H') and Simpson's index of diversity (1-D), Pielou's evenness index (E), and the richness estimator SChao1. As a measure of similarity between the two clone libraries, the Sørensen index (Cs) was also calculated.

Phylogenetic analysis. Representative sequences for each OTU (selected using the "Get.oturep" option in MOTHUR) and DGGE phylotype were used for the 23S rRNA and 16S rRNA gene sequence alignments respectively. In both alignments, similar sequences identified in a BLAST search and sequences from representative species of cyanobacteria available at GenBank were also included. Sequence alignments were performed using MUSCLE 3.8 [19] and manually checked and corrected in BIOEDIT 7.0.52 [29]. To exclude sequence ends and ambiguously aligned regions, Gblocks v.091b [9] was used. To generate a phylogenetic tree, nucleotide substitution models were statistically selected by JMODELTEST [49] [available at http://darwin.uvigo.es]. According to the Akaike information criterion (AIC) [1], the best fitting model of sequence evolution was the General Time Reversible (GTR) substitution model [57] with estimation of invariant sites (+ I) assuming a gamma distribution with six rate categories (+ G). All data sets were analyzed using maximum likelihood and Bayesian inference approaches. Bayesian analyses were performed using the Metropolis coupled Bayesian Markov chain Monte Carlo algorithm $(MC)^3$ implemented in the software MRBAYES v.3.1.2 [34] [http://morphbank.ebc.uu.se/mrbayes]. Analyses $(MC)^3$ for 16S and 23S rRNA gene sequence alignments were run for 8,000,000 and 5,000,000 generations respectively, using a random tree as starting point, 12 simultaneous channels, a temperature of 0.1 and a sampling frequency of 100 generations. The first 20,000 trees for the 16S rRNA alignment and 12,500 trees for the 23S alignment were discarded as burn-in, after verification of the likelihood parameters in TRACER v.1.4 [50]. 50% majority-rule consensus trees were obtained from the remaining trees using the *sumt* option. In addition, maximum likelihood (ML) tests were run in the PhyML 3.0 server [28] [http://www.atgc-montpellier.fr/phyml/] using a non-parametric test with 1000 bootstrap replications to asses branch support [20]. Finally, the resultant phylogenetic trees were visualized with FigTree v.1.3.1 [http://tree.bio.ed.ac.uk/software/figtree/]. *Chloroflexus aggregans* was used as outgroup for the 23S rRNA gene phylogenetic tree while *Deinococcus radiodurans* and *Thermus* sp. were used as outgroups for the 16S rRNA gene phylogenetic tree.

Results

Physico-chemical characterization of ignimbrite rocks. Zones IgW and IgD displayed a similar mineralogical composition as revealed by semiquantitative X-ray analyses. The major mineral phases identified were andesine (48%), sodium disordered anorthite (44%) and biotite (8%). According to the XRF spectra, zones IgW and IgD were practically identical in composition as previously reported for IgD by Wierzchos et al. [62] (Table 1). Based on its chemical composition and total alkali-silica (TAS) diagram [42], which represents the relationship between alkali (wt% of Na_2O + K_2O) and silicate (wt% SiO_2) mineral contents,

Table 1. Chemical composition determined by XRF in terms of major elements (%) of zones with different color, IgD and IgW, in ignimbrite rocks (LOI: Loss of Ignition)

Elements	IgD*	IgW
SiO_2	71.05	72.21
Al_2O_3	14.56	13.66
Fe_2O_3 (total)	1.64	1.49
MnO	0.06	0.06
MgO	0.58	0.54
CaO	1.50	1.60
Na_2O	3.66	2.99
SO_3	0.00	0.39
K_2O	5.12	5.80
TiO_2	0.40	0.38
P_2O_5	0.08	0.07
LOI	1.37	0.81

*Data obtained from Wierzchos et al. [62].

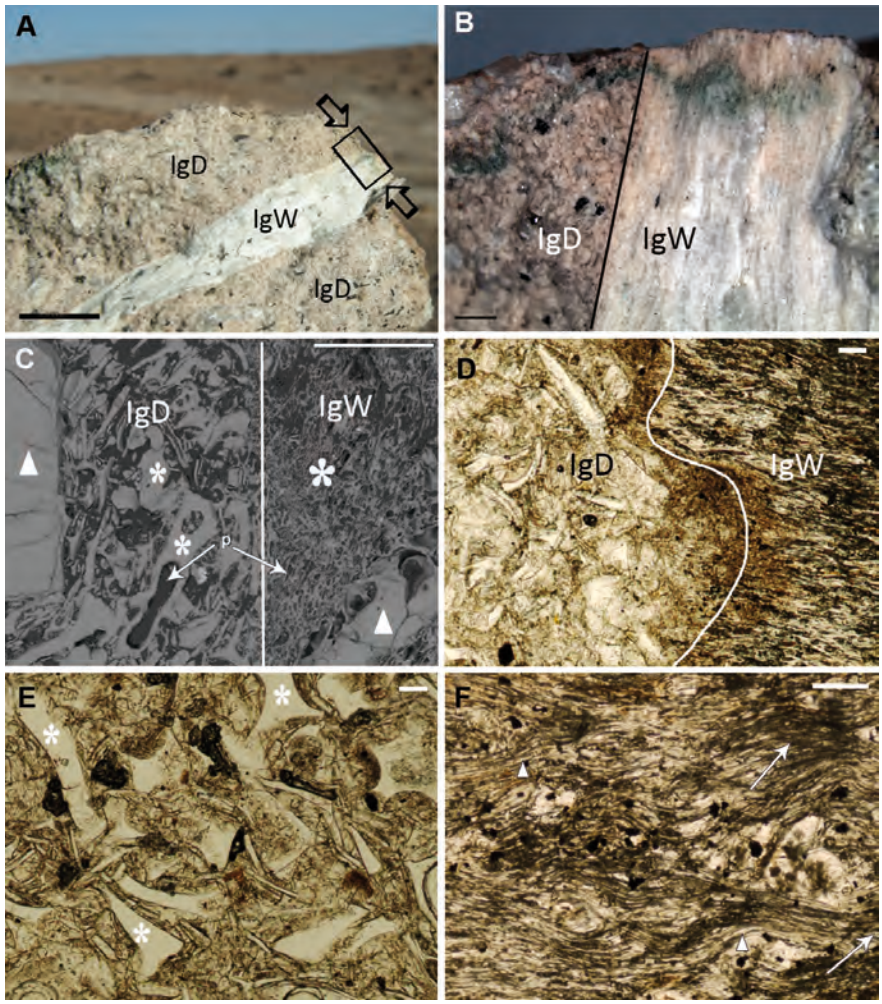

Fig. 2 (**A**) Cross-section of an ignimbrite rock showing the interface between the two defined zones designated IgD (dark ignimbrite) and IgW (white ignimbrite), scale 1 cm. (**B**) Detailed view of Fig. 2(A) (square) showing the IgD/IgW interface and endolithic colonization patterns specific to each zone, scale 1 mm. (**C**) SEM-BSE image of the IgD/IgW interface comprised of a matrix of glass shards (asterisks), plagioclase phenocrysts (triangles) and vesicular pores (p), scale 500 µm. (**D–F**) Plane-polarized light micrographs of IgD and IgW revealing their different textures. (**E**) Matrix of welded glass shards (asterisk) in IgD. And (**F**) matrix of glass shards containing elongated vesicles (arrowheads) in IgW. Note the intense exfoliation pattern defined by the elongated vesicles (arrows). Scales 100 µm from D and E, and 200 µm from F.

the material collected in this study was classified as weakly welded rhyolitic ignimbrite.

The interface between zones IgD and IgW was examined by SEM-BSE and petrographic microscopy (Fig. 2C,D). In the SEM-BSE image (Fig. 2C), both IgD and IgW showed the presence of plagioclase crystals, yet vesicular pores of the matrix of glass fragments in which these were embedded varied in size. This was confirmed by petrographic microscopy observation of the same interface (Fig. 2D).

A detailed view of each zone was obtained by petrographic microscopy (Fig. 2E,F). In these images, it is possible to discern a matrix of glass fragments weakly welded in the beige colored zone (IgD, Fig. 2E) and fragments of glass with small elongated vesicles in the white zone (IgW). This white zone showed intense exfoliation with the exception of areas around the phenocrystals (Fig. 2F).

Zones IgD and IgW were also compared in terms of their porosity and mean and median pore diameters determined by mercury intrusion porosimetry (MIP) (Table 2). These data confirmed our microscopy observations, with zone IgD showing a greater

Table 2. Total porosity, mean and median pore diameter distribution and volume of pores (%) with diameter <1 μm and >1 μm determined by IPM in IgD and IgW

	IgD	IgW
nº samples	4	3
Total porosity (%, volume)	14.4 (± 0.33)	9.65 (± 0.34)
Mean pore diameter (μm)	1.14 (± 0.52)	0.62 (± 0.12)
Median pore diameter (μm)	11.27 (± 1.31)	2.46 (± 0.31)
% Pores with diameter < 1 μm	15.3	29.9
% Pores with diameter > 1 μm	84.7	70.1

total porosity (14%) and mean pore diameter (1.14 ± 0.52 μm). According to Pittman's definition of microporosity [47], the volume of micropores of diameter <1 μm expressed relative to total porosity was higher in IgW (29.9%) than in IgD (15.3%).

Patterns of endolithic colonization. Upon fracturing the ignimbrite rocks, microbial endolithic colonization appeared as a readily discernible green band a few millimeters below the rock surface (zone indicated in Fig. 2A,B). These endolithic communities showed distinct colonization patterns in the zones of different textural properties. In the beige zone IgD, this pattern was a narrow green band (0.5–1 mm thick) at a depth of 1 mm (Fig. 2B), while in IgW, the green band was slightly thicker and more diffuse and dispersed such that its depth ranged from 1 to 2 mm (Fig. 2B).

Photosynthetic microbial composition. Analysis of the 23S rRNA gene. DGGE profiles of the 23S rRNA gene (Fig. 3) contained a small number of bands, and differences were detected between IgD and IgW textures. Eleven DGGE bands were excised, reamplified and sequenced, seven corresponding to IgD (bands a–g) and four to IgW (bands h–k) (Fig. 3 and Table 3). Two of the IgD profiles were identical, while IgD-I showed a unique DGGE profile. Of note, we observed a DGGE band common to all three IgD profiles (a, c and f). High variation was observed in the IgW sample profiles, with the exception of one DGGE band shared between IgW-I (band h) and IgW-III (band k). When comparing profiles according to texture, DGGE profiles for samples IgD-I and IgW-III emerged as identical. IgW showed bands common to the IgD profiles. Similar electrophoretic positions were observed for IgD-I band b, IgW-I band h and IgW-III band k; IgW-II band i, IgD-II band d and IgD-III band g; and IgW-III band j, IgD-I band a, IgD-II band c and IgD-III band f. Four different phylotypes (I, II, III and IV) were defined based on ≥99% sequence similarity. Three of these phylotypes were detected in both ignimbrite textures, while phylotype IV only appeared in one IgD profile (Table 3). Based on 97% and

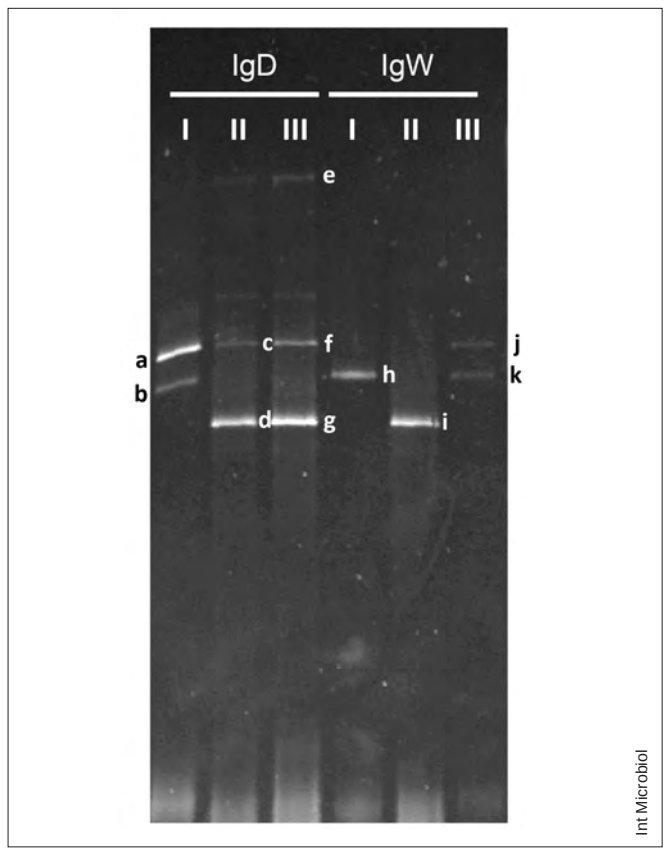

Fig. 3. DGGE profiles of PCR-amplified 23S rRNA gene fragments (404 bp) derived from representative samples of the green bands of endolithic colonization in zones IgD and IgW (IgD dark ignimbrite, IgW white ignimbrite). Three samples of each texture (zone) were analyzed (I-III). Letters a-k indicate DGGE bands that were excised, reamplified, purified and sequenced for analysis (see Table 3).

.

Table 3. DGGE bands of 23S rRNA gen from the IgD and IgW textures of ignimbrite rocks indicated in Fig. 3, and BLAST analysis of the obtained phylotypes (based on sequence similarity ≥99%)

DGGE Bands	Phylotype	IgD	IgW	Closest GenBank sequences, (accession number), % similarity	Location	Closest sequecens of identified organisms in GenBank (accession number), % similarity
a, c, f, j	I	✓	✓	Uncultured bacterium isolate DGGE gel band A (JQ700570), 99% ; band B (JQ700571), 98% Uncultured *Chroococcidiopsis* clone A1.1, NA4.3 (FJ805915, FJ805885), 98%	Atacama Desert, Chile Lybian Desert, Egypt Death Valley, USA	*Microcoleous chthonoplastes* (AM709630), 91%
b, h, k	II	✓	✓	Uncultured *Chroococcidiopsis* clone AS5.13-8-5 (FJ805955-50, 47), 99%	Turpan Depression, China	*Lyngbya aestuarii* PCC 7419 (AY584522), 91%
d, g, i	III	✓	✓	Uncultured bacterium isolate DGGE gel band B (JQ700571), 100%; band A, (JQ700570), 98% Uncultured *Chroococcidiopsis* clone A1.1, NA4.3 (FJ805915, FJ805885), 97%	Atacama Desert, Chile Lybian Desert, Egypt Death Valley, USA	*Thermosynechococcus sp.* NK55 (CP006735), 93%
e	IV	✓		Uncultured bacterium isolate DGGE gel band B (JQ700571) 99%; band A (JQ100570), 99% Uncultured *Chroococcidiopsis* clone A1.1, NA4.3 (FJ805915, FJ805885) 98%	Atacama Desert, Chile Lybian Desert, Egypt Death Valley, USA	*Thermosynechococcus* sp. NK55 (CP006735), 92%

95% sequence similarities, two potential species and two potential genera (Genera 1 and 2) were differentiated in IgD and IgW, one species included in Genera 1 (Phylotypes I, III and IV), and the remaining species in Genera 2 (Phylotype II).

BLAST analysis of the recovered phylotypes indicated they were all cyanobacteria showing most sequence similarity with uncultured bacterial isolates from the Atacama Desert (Chile) and uncultured hypolithic members of the *Chroococcidiopsis* genus from other extreme hyper-arid environments (Lybian Desert, Egypt, and Death Valley, USA). Sequences closest to organisms from the GenBank database were those of *Microcoleus chthonoplastes*, *Thermosynechococcus* sp. and *Lyngbya aestuarii* (showing 91–93% similarity, Table 3).

Our 23S rRNA gene sequence alignment showed a final size of 406 nucleotide positions, including gaps and a total of 54 sequences. The phylogenetic positions of the phylotypes corresponding to the DGGE bands were resolved by Bayesian inference and maximum likelihood methods, yielding consensus trees with the same topology (Fig. 4). The 50% majority-rule consensus tree showed that the DGGE phylotypes (pink color in Fig. 4) clustered with two uncultured bacteria isolated in a previous investigation from IgD ignimbrite rocks [62] and with different uncultured hypolithic clones of *Chroococcidiopsis* cyanobacteria from hot arid deserts (Turpan Depression, China; Desert Dubai, United Arab Emirates; Desert Death Valley, USA; Atacama Desert, Chile in Bahl et al. [3]). The latter sequences correspond to the "HOT DESERT I" and "HOT DESERT II" groups designated by Bahl et al. [3]. Phylotype II was detected in "HOT DESERT II" with a *posterior* probability (PP) = 99% and bootstrap probability (BP) = 94.9%; remaining phylotypes (I, III and IV) clustered with sequences belonging to the "HOT DESERT I" group.

Analysis of 16S rRNA gene. In total, 96 clones were obtained from both libraries (IgD and IgW), of which 73 clones provided high quality sequences, 37 from IgD and 36 from IgW. According to the criteria that sequence similarities >97% and >95% correspond to similar species or genera, respectively, the sequences obtained in this study indicated three OTUs in each library. At the species level, two OTUs were

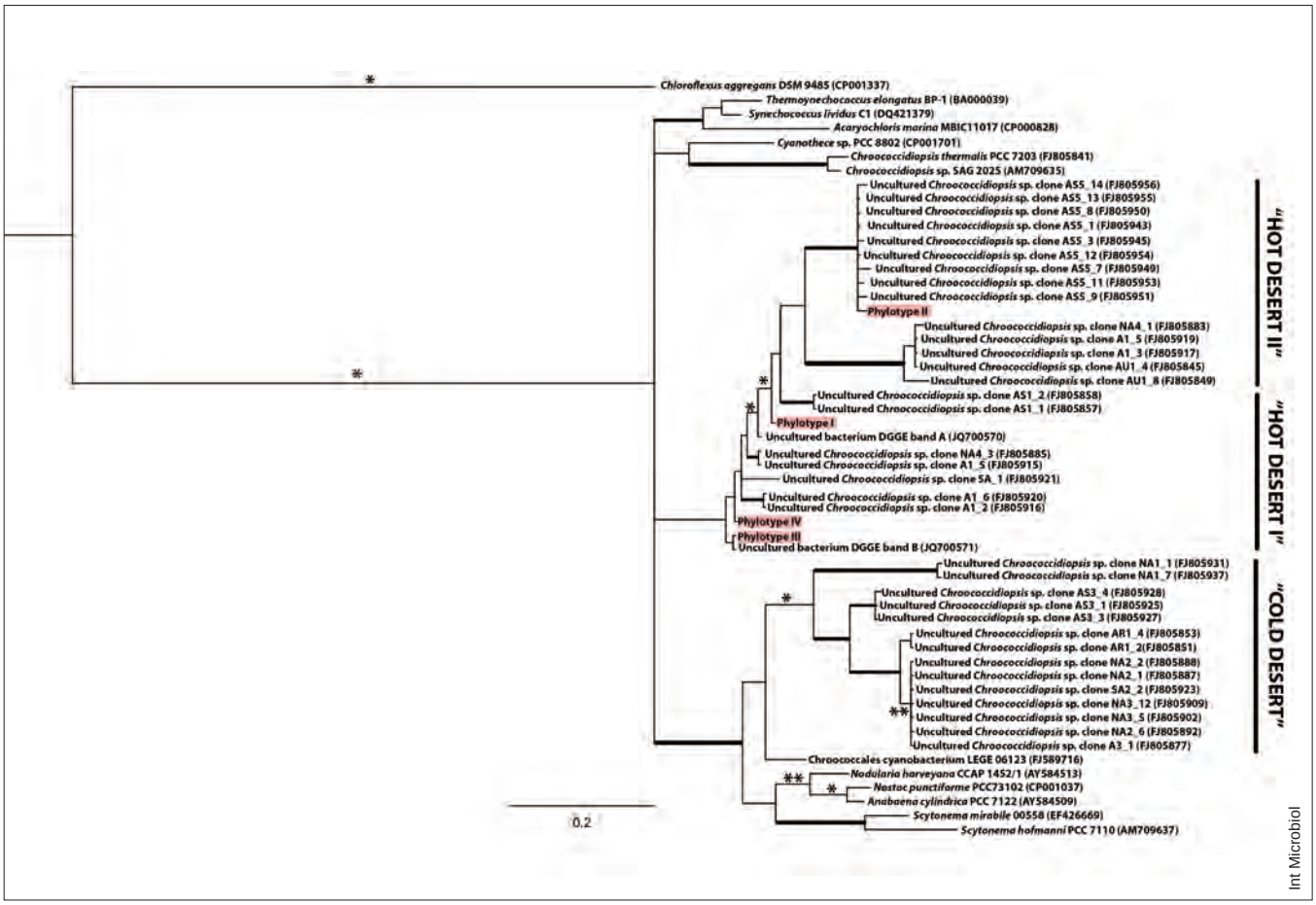

Fig. 4.Consensus phylogenetic tree (50%-majority rule) based on the 23S rRNA gene region (406 pb) reconstructed using Bayesian inference and maximum likelihood to infer the phylogenetic positions of the DGGE phylotypes recovered from zones IgD and IgW (indicated in pink). Branches in bold are supported by both methods with Bayesian *posterior* probability (PP) ≥ 95% and bootstrap probability (BP) > 70%. One asterisk indicates a branch supported only by PP, and two asterisks a branch supported only by BP. *Chloroflexus aggregans* was used as outgroup. In the right margin of the figure, we provide the groups designated by Bahl et al. [3] for uncultured *Chroococcidiopsis* hypolithic clones from hot and cold arid deserts.

common to IgD and IgW (OTU-1 and OTU-2), while the remaining OTUs of each library were unique to one or other zone (OTU-3: IgD and OTU-4: IgW). At the genus level, three OTUs were also recovered (OTU-A, OTU-B, OTU-C) in both ignimbrite zones: OTU-A including OTU-1, OTU-B including OTU-2, and OTU-C including OTU-3 and OTU-4.

In terms of relative abundances of each OTU at the species level, the most abundant OTUs were OTU-1 (59%) and OTU-3 (38%) in the IgD library and OTU-1 (61%) and OTU-4 (36 %) in the IgW library, OTU-2 being in both cases the OTU with the lowest number of sequences (2%).

Our statistical analysis revealed 97% coverage and similar indices of diversity and evenness in both libraries. The Shannon index (H') and Simpson index of diversity (1-D) were low in terms of richness and abundance (H'_{IgD} = 0.774 and H'_{IgW} =0.768; 1-D_{IgD} = 0.517 and 1-D_{IgW} = 0.509) in both libraries. Pielou's index revealed a tendency towards evenness in both libraries (0.705 in IgD and 0.699 in IgW). In addition, the estimator SChao1 indicated low, identical species richness for IgW and IgD (3 in both cases). This similarity between the two libraries was also supported by the Sorensen index (Cs = 0.67).

BLAST analysis of the most representative sequences of each OTU obtained at the species level revealed their greater similarity with sequences of uncultured hypolithic bacterium clones, most related to the *Chroococcidiopsis* genus. Further, sequences also displayed 93–98% similarity to that of the closest identified organism from the GenBank database (Table 4). The alignment of 16S rRNA gene sequences resulted in a final size of 604 nucleotide positions, including gaps, with a total of 50 sequences. In the consensus tree (Fig. 5), common OTUs to IgD and IgW appeared in two distinct clades (OTU-1 supported by PP = 98%, OTU-2 supported by PP = 99% and

Table 4. OTUs identity obtained from clone libraries (16S rRNA gene) from the IgD and IgW ignimbrite textures

OTUs[a]	IgD	IgW	Closest GenBank sequences, (accession number), % similarity	Closest sequecens of identified organisms in GenBank (accession number), % similarity
OTU-1	(22)[b]	(22)	Uncultured bacterium clone 151 (HM241016) 97%	*Chroococcidiopsis* CC1 (DQ914863) 93%
OTU-2	(1)	(1)	Uncultured bacterium clone 225 (HM241090) 99%	*Chroococcidiopsis* CC3 (DQ914865) 98%
OTU-3	(14)		Uncultured bacterium clone 157 (HM241022) 98%	*Chroococcidiopsis* CC3 (DQ914865) 95%
OTU-4		(13)	Uncultured bacterium clone 186 (HM241051) 98%	*Chroococcidiopsis* CC3 (DQ914865) 94%

[a]The definition of OTUs (at the species level) was based on a sequence similarity > 97% for phylogenetic analysis.
[b]Numbers indicate the number of sequences included in each OTU.

BP = 93.9%), clustering cyanobacterial sequences from the *Chroococcidiopsis* genus and from hypolithic cyanobacteria isolated from arid extreme environments, including sequences corresponding to the Yungay area of the Atacama Desert. The taxonomic affiliations of OTU-3 and OTU-4, unique to each library, were not completely resolved. Both OTUs clustered in the same clade, along with sequences of hypolithic microorganisms from deserts and sequences of the *Oscillatoriales* order, but without statistical support.

Discussion

Volcanic rocks from the Atacama Desert are ideal models to explore microbial adaptation strategies in extreme arid environments. In a previous work it was shown that the ignimbrite rock interior provides protection from damaging UV radiation and excessive visible light [62]. This work is extended to assess the textural properties of ignimbrite as a determining factor for endolithic microbial colonization patterns. Cyanobacteria were detected as the main colonizers of the interior of weakly welded rhyolitic ignimbrite rocks collected from the Preandean Depression area of the Atacama Desert, where environmental conditions are stubbornly dry. Note that many rock fragments showed two well-differentiated micromorphological zones of different texture yet identical chemical and mineralogical composition (IgD and IgW). The novelty of the present work lies in the differences detected in patterns of cyanobacterial colonization and composition between these two zones.

The different microbial colonization patterns observed in IgD (beige zone) and IgW (white zone) could be correlated with the porosity and color of each zone given their practically identical chemistry. Endolithic colonization patterns have been related to the intrinsic properties of building materials such as dolostone and granite [8,22,27,44]. The textural differences detected here between IgD and IgW were mainly due to their petrophysical properties, total porosity, pore size distribution and shape and orientation of pores. These features are known to influence water movement through the rock matrix along with water retention. In our study, the greater proportion of micropores detected in IgW (29.9%), their tubular shape and parallel orientation to the rock surface could be responsible for the more diffuse and deeper green band of microbial colonization observed compared to the thinner band observed for IgD. Micropores could have a greater water retention capacity and reduced evaporation rate, because, after a wetting event they can trap and more easily retain water than larger pores [44,46,58,60,62]. According to Omelon et al. [46], the presence of water in micropores, especially those with translucent walls such as ignimbrite pores, can enhance light penetration and therefore increase the light available for photosynthesis in the cryptoendolithic habitat [46].

In addition, the lighter color of the IgW zone, probably attributable to its smaller proportions of total Fe (Table 1), could also lead to higher light transmittance through this texture [43]. Factors such as porosity and light distribution have been shown to play a key role in microbial community structure in polar deserts [46,48] and other environments [31,43,56], and may differ at the microscale level.

Both clone libraries and DGGE gels revealed a low number of cyanobacterial phylotypes in our rock samples, most of which were related to the genus *Chroococcidiopsis*, suggesting a very low diversity of photosynthetic microorganisms. Three cyanobacterial phylotypes (I, II and III) common to both ignimbrite zones and one phylotype (IV) only present in IgD

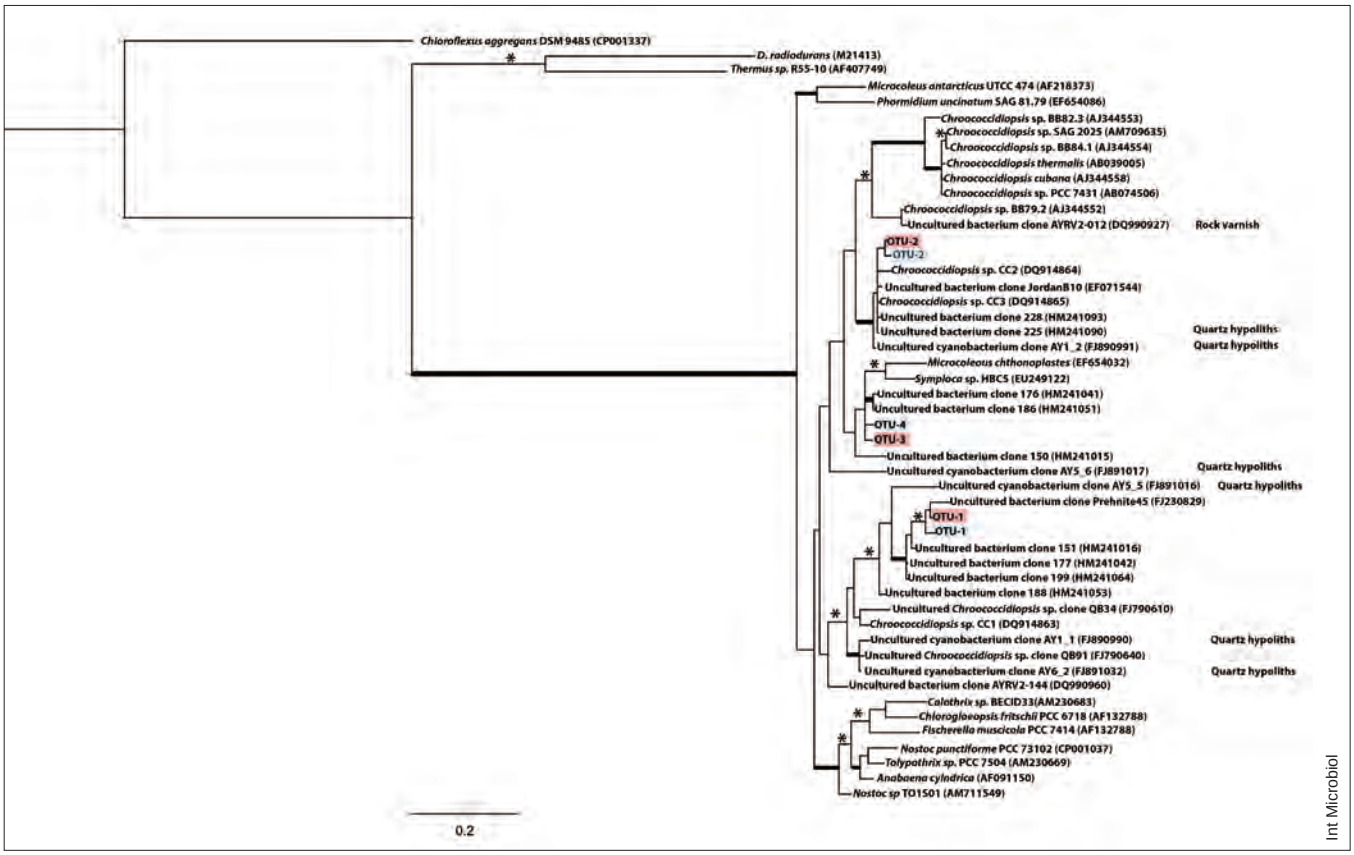

Fig. 5. Consensus phylogenetic tree (50%-majority rule) based on the 16S rRNA gene region (604 pb) reconstructed using Bayesian inference and maximum likelihood to infer the phylogenetic positions of the OTUs recovered from the Ig clone libraries (IgD pink, IgW blue). Branches in bold are supported by both methods with Bayesian posterior probability (PP) ≥ 95% and bootstrap probability (BP) > 70%. One asterisk indicates a branch supported only by PP, and two asterisks a branch supported only by BP. *Chloroflexus aggregans*, *Deinococcus radiodurans* and *Thermus* sp. sequences were used as outgroups. In the right margin of the figure, we provide sequences generated in previous studies on microbial communities of the Atacama Desert.

were detected by DGGE and led to the identification of two potential species from distinct genera. In addition, our clone libraries revealed four OTUs of three different genera, one more than those detected through DGGE. Two of these taxonomic units (OTU-1 and OTU-2) were common to both textures and the other two were unique to IgD (OTU-3) or IgW (OTU-4). The latter represented a high proportion of clones in their corresponding textures and clustered in the same clade in the 16S rRNA phylogenetic tree, indicating their same genus but different species. The taxonomic affiliations of OTU-3 and OTU-4 could not be resolved though they seemed to be related to two *Oscillatoria* strains. In a phylogenetic study of *Chroococcidiopsis* taxa, two oscillatorian strains have been found to cluster with statistical support within *Chroccoccidiopsis* (Donne 2013, PhD dissertation). According to the authors of this study, during phylogenetic analysis hyper-variable regions important for the separation of *Chroococcidiopsis* and these oscillatorian taxa could have been removed in the multi-sequence alignment. In effect, the 16S rRNA gene is commonly used as genetic marker for the phylogenetic analysis of cyanobacteria, but this marker is sometimes not able to resolve relationships among very closely related organisms [35].

The detection of different phylotypes in the two micromorphological ignimbrite zones suggests cyanobacterial composition variations across a small spatial scale associated with different textures. Such microvariations in cyanobacterial diversity could be attributable to slightly different conditions in terms of availability of water and light. Further work is needed, including light transmittance measurements, to address this hypothesis.

To confirm the idea that cyanobacteria were the only phototrophic microorganisms comprising the microbial communities detected, we also assessed the presence of eukaryotic microorganisms using different primer set and PCR condition combinations (data not shown), though no amplification products were obtained. Moreover, neither could we detect DGGE

bands corresponding to algae. Wierzchos et al. [62] reached a similar conclusion after their microscopy analysis of IgD rock samples from the same region.

Cyanobacteria are ubiquitous in the volcanic rocks of many terrestrial environments [11,23,31,36,37]. However, in early successional volcanic communities such as those found in lava flows following the recent eruption of a volcano in southern Iceland, phototrophy is not thought to be a dominant biogeochemical process [38]. Considering the Pliocene and Upper Miocene [17,21] age of the ignimbrite rocks of the Preandean Depression area of the Atacama Desert, an early successional stage for the endolithic communities examined here can be ruled out especially since cyanobacteria are the main photosynthetic members of these microbial communities.

The presence of the genus *Chroococcidiopsis* as a component of the photosynthetic endolithic community in Lomas de Tilocalar is not surprising. Several studies have identified periodic desiccation as one of the most determining factors for microbial colonization of terrestrial volcanic rocks mainly comprising desiccation resistant or spore forming microorganisms [11]. *Chroococcidiopsis* spp. are known for their ability to withstand long desiccation periods [25] and cell damage by UV radiation [6], which makes this group of prokaryotes among the best-adapted to desert conditions [6,25]. The present findings broaden the spectrum of Atacama Desert rock substrates in which the presence of *Chroococcidiopsis* has been detected [18,39,40, 62].

The cyanobacterial phylotypes detected in our ignimbrite samples (IgD and IgW) were unrelated to endolithic and epilithic phylotypes recovered from other volcanic rocks [12,23,31,32,36–38]. In fact, most of the sequences obtained in this study showed most similarity with sequences of *Chroococcidiopsis* hypolithic clones from arid hot deserts including the Atacama Desert, Death Valley, Turpan Depression and Lybian Desert [3]. This suggests that microorganisms inhabiting the cryptoendolithic microhabitat of ignimbrite and hypolithic microhabitat of quartz are subjected to similar selective pressures giving rise to highly specialized microorganisms able to withstand long periods of desiccation. In effect, the potential for endolithic behavior of Antarctic hypolithic microorganisms has been recently shown [14].

In conclusion, the present findings contribute to the current understanding of the microbial diversity of both hot arid deserts and volcanic rocks, and identify subtle physico-chemical rock properties as determinants of microbial colonization patterns. Our findings provide direction for future studies, involving a greater sampling effort and high-throughput technologies, designed to gain further insight into endolithic microbial diversity and the impacts of textural features on this diversity and ecosystem functioning.

Acknowledgments. The authors thank F. Pinto, V. Souza-Egipsy, and T. Carnota for help with the SEM-BSE observations, M.J. Malo for help with the molecular biology techniques, R. Gonzalez and M. Juanco for help with the MIP work, D. Herrera for help with sample collection in the Atacama Desert, Ana Burton for editorial assistance and reviewers for their constructive comments. This study was supported by grants CGL2010-16004 and CTM2012-38222-C02-02 and CGL2013-42509 from the Spanish Ministry of Economy and Competitiveness and by a predoctoral FPI fellowship program (BES-2007-15145).

Competing interests. None declared.

References

1. Akaike H (1974) A new look at the statistical model identification. IEEE Trans Automat Contr 19:716-723
2. Antony CP, Shimpi GG, Cockell CS, Patole MS, Shouche YS (2014) Molecular characterization of prokaryotic communities associated with lonar crater basalts. Geomicrobiol J 31:519-528
3. Bahl J, Lau MCY, Smith GJD, Vijaykrishna D, Cary SC, Lacap DC, Lee CK, Papke RT, et al. (2011) Ancient origins determine global biogeography of hot and cold desert cyanobacteria. Nat Commun 2:163
4. Barker PE, Rea WJ, Skarmeta J, Caminos R, Rex DC (1981) Igneous history of the Andean cordillera and Patagonian plateau around latitude 46ºS. Philos T R Soc S-A 303:105-149
5. Benavente D, García Del Cura MA, Ordóñez S (2003) Salt influence on evaporation from porous building rocks. Constr Build Mater 17:113-122
6. Billi D, Viaggiu E, Cockell CS, Rabbow E, Horneck G, Onofri S (2011) Damage escape and repair in dried *Chroococcidiopsis* spp. from hot and cold deserts exposed to simulated space and Martian conditions. Astrobiology 11:65-73
7. Büdel B, Weber B, Kühl M, Pfanz H, Sültemeyer D, Wessels DC (2004) Reshaping of sandstone surfaces by cryptoendolithic cyanobacteria: bioalkalinization casuses chemical weathering in arid landscapes. Geobiology 2:261-268
8. Cámara B, De Los Ríos A, García Del Cura MÁ, Galvan V, Ascaso C (2008) Dolostone bioreceptivity to fungal colonization. Mater Construcc 58:113-124
9. Castresana J (2000) Selection of conserved blocks from multiple alignments for their use in phylogenetic analysis. Mol Biol Evol 17:540-552
10. Chung FH (1974) Quantitative interpretation of X-ray-diffraction patterns of mixtures. 2. Adiabatic principle of X-ray-diffraction analysis of mixtures. J Appl Crystallogr 7:526-531
11. Cockell CS, Kelly LC, Summers S (2011) Microbiology of volcanic environments. In: Horikoshi K, Antranikian, G., Bull, AT, Robb, FT, Stetter, KO (eds) Extremophiles handbook. Springer Verlag, Berlin, pp. 917-933
12. Cockell CS, Olsson K, Knowles F, Kelly LC, Herrera A, Thorsteinsson T, Marteinsson V (2009b) Bacteria in weathered basaltic glass, Iceland. Geomicrobiol J 26:491-507

13. De los Rios A, Bustillo A, Ascaso C, Carvalho M R (2011) Bioconstruction in ochreous speleothems from lava on Terceira Island (Azores). Sediment Geol 236:117-128
14. De los Rios A, Cary G, Cowan D (2014) The spatial structures of hypolithic communities in the Dry Valley of East Antarctica. Polar Bio. doi:10.1007/s00300-014-1564-0
15. De Los Rios A, Valea S, Ascaso C, Davila A, Kastovsky J, Mckay CP, Gomez-Silva B, Wierzchos J (2010) Comparative analysis of the microbial communities inhabiting halite evaporites of the Atacama Desert. Int Microbiol 13:79-89
16. De Los Ríos A, Wierzchos J, Sancho LG, Ascaso C (2003) Acid microenvironments in microbial biofilms of Antarctic endolithic microecosystems. Environ Microbiol 5:231-237
17. De Silva SL (1989) Geochronology and stratigraphy of the ignimbrites from the 21º30'S to 23º30′S portion of the central Andes of northern Chile. J Volcanol Geoth Res 37:93-131
18. DiRuggiero J, Wierzchos J, Robinson CK, Souterre T, Ravel J, Artieda O, Souza-Egipsy V, Ascaso C (2012) Microbial colonization of chasmoendolithic habitats in the hyper-arid zone of the Atacama Desert. Biogeosci Discuss 9:15603-15632
19. Edgar RC (2004) MUSCLE: multiple sequence alignment with high accuracy and high throughput. Nucleic Acids Res 32:1792-1797
20. Felsenstein J (1985) Confidence limits on phylogenies: an approach using the bootstrap. Evolution 39:783-791
21. Gardeweg PM, Ramirez CF (1987) The La Pacana Caldera and the Atana ignimbrite: a major ash-flow and resurgent caldera complex in the Andes of northern Chile. B Volcanol 49:547-566
22. Gleeson DB, Clipson N, Melville K, Gadd GM, Mcdermott FP (2005) Characterization of fungal community structure on a weathered pegmatitic granite. Microb Ecol 50:360-368
23. Gomez-Alvarez V, King G, Nüsslein K (2007) Comparative bacterial diversity in recent Hawaiian volcanic deposits of different ages. FEMS Microbiol Ecol 60:60-73
24. González G, Cembrano J, Aron F, Veloso EE, Shyu JBH (2009) Coeval compressional deformation and volcanism in the central Andes, case studies from northern Chile (23ºS–24ºS). Tectonics 28 doi:10.1029/2009TC002538
25. Grilli Cariola M, Ocampo-Friedmann R, Friedmann EI (1993) Cytology of long-term desiccation in the desert cyanobacterium *Chroococcidiopsis* (Chroococcales). Phycologia 32:315-322
26. Guest JE (1969) Upper Tertiary ignimbrites in Andean cordillera of part of Antofagasta province northern Chile. Geol Soc Am Bull 80:337-364
27. Guillitte O (1995) Bioreceptivity: a new concept for building ecology studies. Sci Total Environ 1995:215-220
28. Guindon S, Dufayard J, Lefort V, Anisimova M, Hordijk W, Gascuel O (2010) New algorithms and methods to estimate maximum-likelihood phylogenies: Assessing the performance of PhyML 3.0. Syst Biol 59:307-321
29. Hall TA (1999) BioEdit: a user-friendly biological sequence alignment editor and analysis program for Windows 95/98/NT. Nucl Acid S Series 41:95-98
30. Hathaway JJM, Garcia MG, Balasch MM, Spilde MN, Stone FD, Dapkevicius MLNE, Amorim IR, Gabriel R, Borges PAV, Northup DE (2014) Comparison of bacterial diversity in Azorean and Hawaiian Lava Cave microbial mats. Geomicrobiol J 31:205-220
31. Herrera A, Cockell CS, Self S, Blaxter M, Reitner J (2009) A cryptoendolithic community in volcanic glass. Astrobiology 9:369-381
32. Herrera A, Cockell CS, Self S, Blaxter M, Reitner J, Arp G, Dröse W, Thorsteinsson T, et al (2008) Bacterial colonization and weathering of terrestrial obsidian in Iceland. Geomicrobiol J, 25:25-37
33. Huber T, Faulkner G, Hugenholtz P (2004) Bellerophon: a program to detect chimeric sequences in multiple sequence alignments. Bioinformatics 20:2317-2319.
34. Huelsenbeck JP, Ronquist F (2001) MrBayes: Bayesian Inference of phylogenetic trees. Bioinformatics 17:754-755
35. Kauff F, Büdel B (2011) Molecular phylogeny in the cyanobacteria. Prog Bot 72:209-224
36. Kelly LC, Cockell CS, Thorsteinsson T, Marteinsson V, Stevenson J (2014) Pioneer microbial communities of the Fimmvorethuhals lava flow, Eyjafjallajokull, Iceland. Microb Ecol. doi:10.1007/s00248-014-0432-3
37. Kelly LC, Cockell CS, Piceno YM, Andersen GL, Thorsteinsson T, Marteinsson V (2010) Bacterial diversity of weathered terrestrial Icelandic volcanic glasses. Microb Ecol 60:740-752
38. Kelly LC, Cockell CS, Herrera-Belaroussi A, Piceno Y, Andersen G, Desantis T, Brodie E, Thorsteinsson T, et al. (2011) Bacterial diversity of terrestrial crystalline volcanic rocks, Iceland. Microb Ecol 62:69-79
39. Kuhlman K, Venkat P, La Duc M, Kuhlman G, Mckay C (2008) Evidence of a microbial community associated with rock varnish at Yungay, Atacama Desert, Chile. J Geophys Res Biogeosci 113.
40. Lacap DC, Warren-Rhodes KA, Mckay CP, Pointing SB (2010) Cyanobacteria and chloroflexi-dominated hypolithic colonization of quartz at the hyper-arid core of the Atacama Desert, Chile. Extremophiles 15:31-38
41. Lane D (1991) 16S/23S rRNA Sequencing. In: Stackebrand E, Goodfellow M (eds) Nucleic acid techniques in bacterial systematics, John Wiley & Sons
42. Le Bas MJ, Le Maitre RW, Woolley AR (1992) The construction of the total alkali-silica chemical classification of volcanic rocks. Miner Petrol 46:1-22
43. Matthes U, Turner SJ, Larson DW (2001) Light attenuation by limestone rock and its constraint on the depth distribution of endolithic algae and cyanobacteria. Int J Plant Sci 162:263-270
44. Miller AZ, Sanmartin P, Pereira-Pardo L, Dionisio A, Saiz-Jimenez C, Macedo MF, Prieto B (2012) Bioreceptivity of building stones: a review. Sci Total Environ 426:1-12
45. Olsson-Francis K, Simpson AE, Wolff-Boenisch D, Cockell CS (2012) The effect of rock composition on cyanobacterial weathering of crystalline basalt and rhyolite. Geobiology 10:434-444
46. Omelon CR (2008) Endolithic microbial communities in polar desert habitat. Geomicrobiol J 25:404-414
47. Pittman ED (1971) Microporosity in carbonate rocks. Am Assoc Petr Geol B 55:1873-1881.
48. Pointing SB, Chan Y, Lacap DC, Lau MCY, Jurgens JA, Farrell RL (2009) Highly specialized microbial diversity in hyper-arid polar desert. Proc Natl Acad Sci USA 106:19964-19969
49. Posada D (2008) jModelTest: Phylogenetic model averaging. Mol Biol Evol 25:1253-1256
50. Rambaut A, Drummond AJ (2007) Tracer v1.4. Available at http://beast.bio.ed.ac.uk/Tracer
51. Ramírez CF, Gardeweg M (1984) Hoja Toconao, Región de Antofagasta, 1:250.000, Carta 54. Geología Chile Servicio Nacional de Geología y Mineralogía Santiago, 122 pp
52. Robinson CK, Wierzchos J, Black C, Crits-Christoph A, Ma B, Ravel J, Ascaso A, Artieda O, et al. (2014) Microbial diversity and the presence of algae in halite endolithic communities are correlated to atmospheric moisture in the hyper-arid zone of the Atacama Desert. Environ Microbiol. doi:10.1111/1462-2920.12364
53. Rosselló-Mora R, Amann R (2001) The species concept for prokaryotes. FEMS Microbiol Rev 25:39-76

54. Schloss PD, Westcott SL, Ryabin T, Hall JR, Hartmann M, Hollister EB, Lesniewski RA, Oakley BB, et al. (2009) Introducing mothur: Open-source, platform-independent, community-supported software for describing and comparing microbial communities. Appl Environ Microb 75:7537-7541
55. Sherwood AR, Presting GG (2007) Universal primers amplify a 23S rDNA plastid marker in eukaryotic algae and cyanobacteria. J Phycology 43:605-608
56. Sigler W, Bachofen R, Zeyer J (2003) Molecular characterization of endolithic cyanobacteria inhabiting exposed dolimite in central Switzerland. Environ Microbiol 5:618-627
57. Tavare S (1986) Some probabilistic and statistical problems in the analysis of DNA sequences. Lectures Math Life Sci 17:57-86
58. Warscheid T, Braams J (2000) Biodeterioration of stone: a review. Int Biodeter Biodegr 46:343-368
59. Warscheid T, Oelting M, Krumbein WE (1991) Physico-chemical aspects of biodeterioration processes on rocks with special regard to organic pollutants. Int Biodeter 28:37-48
60. Warscheid T, Becker T, Braams J, Brüggerhoff S, Gehrmann C, Krumbein WE, Petersen K (1993) Studies on the temporal development of microbial infection of different types of sedimentary rocks and its effect on the alteration of the physico-chemical propierties in building material. In: Thiel M-J (ed) Conservation of stone and other materials Vol. I. E & FN, London (UK)
61. Wierzchos J, Ascaso C (1994) Application of back-scattered electron imaging to the study of the lichen-rock interface. J Microsc 175:54-59
62. Wierzchos J, Davila AF, Artieda O, Cámara-Gallego B, De Los Ríos A, Nealson KH, Valea S, García-González MT, et al. (2013) Ignimbrite as a substrate for endolithic life in the hyper-arid Atacama Desert: Implications for the search for life on Mars. Icarus 224:334-346
63. Wierzchos J, Cámara B, De Los Ríos A, Davila AF, Sánchez Almazo IM, Artieda O, Wierzchos K, Gómez-Silva B, et al. (2011) Microbial colonization of Ca-sulfate crusts in the hyper-arid core of the Atacama Desert: implications for the search for life on Mars. Geobiology 9:44-60